

Growth of a Vortex Mode during Gravitational Collapse Resulting in Type II Supernova

Tomoyuki Hanawa

Department of Astrophysics, School of Science, Nagoya University, Chikusa-ku, Nagoya 464-8602, Japan

hanawa@a.phys.nagoya-u.ac.jp

and

Tomoaki Matsumoto

Department of Humanity and Environment, Hosei University, Fujimi, Chiyoda-ku, Tokyo 102-8160, Japan

matsu@i.hosei.ac.jp

ABSTRACT

We investigate stability of a gravitationally collapsing iron core against non-spherical perturbation. The gravitationally collapsing iron core is approximated by a similarity solution for dynamically collapsing polytropic gas sphere. We find that the similarity solution is unstable against non-spherical perturbations. The perturbation grows in proportion to $(t - t_0)^{-\sigma}$ while the central density increases in proportion to $(t - t_0)^{-2}$. The growth rate is $\sigma = 1/3 + \ell(\gamma - 4/3)$, where γ and ℓ denote the polytropic index and the parameter ℓ of the spherical harmonics, $Y_\ell^m(\theta, \varphi)$, respectively. The growing perturbation is dominated by vortex motion. Thus it excites global convection during the collapse and may contribute to material mixing in a type II supernova.

Subject headings: gravitation — hydrodynamics — instabilities — stars: supernovae

1. INTRODUCTION

Supernova remnants are appreciably aspherical and globally asymmetric. The asymmetry of ejecta indicates that the supernova explosion is highly non-spherical and contains non-radial flow (see, e.g., the review by Goldreich, Lai & Sahrting 1997 and references therein). The non-radial flow in supernova explosion is suggested also from x-ray and γ -ray observations of SN1987A; one cannot explain early detection of x-rays and γ -rays from SN1987A without invoking large scale mixing (see, e.g., the review by Bethe 1990 and the references therein). The origin of high velocity

pulsars may also be ascribed to asymmetry of supernova explosion (see, e.g., Burrows & Hayes 1996 and references therein).

Asymmetry is amplified by the Rayleigh-Taylor instability in the early phase of supernova explosion (see, e.g., Falk & Arnett 1973). According to detailed numerical simulations, the growth of the Rayleigh-Taylor instability accounts for matter mixing inferred from observations of SN1987A if there exists an appropriate seed of the asymmetry (Arnett, Fryxell, & Müller 1989; Hachisu et al. 1990; Müller, Fryxell, & Arnett 1991; Fryxell, Arnett, & Müller 1991; Nagataki, Shimizu, & Kato 1998). Thus it is worth to consider the origin for the seed of asymmetry.

Goldreich et al. (1997) discussed possible instabilities during the core collapse as a source of the seed. They suggested possibility that dynamically collapsing core might be unstable against non-radial perturbation and proposed to study the stability of the similarity solution of Yahil (1983). Applying the polytropic equation of state, $P = K\rho^\gamma$, to pre-supernova core, he obtained a similarity solution describing collapse of a spherical iron core. In this paper we show that his similarity is indeed unstable against a vortex mode. The method of stability analysis is essentially the same as that of Hanawa & Matsumoto (2000) who investigated the bar mode instability during collapse prior to protostar formation. Velocity perturbation dominates over density perturbation in the vortex mode while both of them have similar amplitude in the bar mode. The growth rate of the vortex mode depends on the wavenumber, ℓ , of the spherical harmonics, $Y_\ell^m(\theta, \varphi)$. The vortex mode grows in proportion to $|t - t_0|^{-\sigma}$, where t_0 and $\sigma = 1/3 + \ell(\gamma - 4/3)$ denote the epoch of protoneutron star and growth rate, respectively.

In §2 we review the similarity solution of Yahil (1983) for our stability analysis given in §3. We discuss the mechanism of the vortex mode in §4 and implications to type II supernova in §5. We show the asymptotic behavior of the similarity solution and perturbation in the region very far from the center in Appendix.

2. SIMILARITY SOLUTION

For simplicity we consider gas of which equation of state is expressed by polytrope,

$$P = K \rho^\gamma, \tag{1}$$

where P and ρ denote the pressure and density, respectively. The hydrodynamical equations are then expressed as

$$\frac{\partial \rho}{\partial t} + \nabla \cdot (\rho \mathbf{v}) = 0 \tag{2}$$

and

$$\frac{\partial}{\partial t}(\rho \mathbf{v}) + \nabla P + \nabla \cdot (\rho \mathbf{v} \otimes \mathbf{v}) + \rho \nabla \Phi = 0, \tag{3}$$

where \mathbf{v} and Φ denote the velocity and gravitational potential, respectively. The gravitational potential is related with the density distribution by the Poisson equation,

$$\Delta\Phi = 4\pi G\rho, \quad (4)$$

where G denotes the gravitational constant.

For later convenience, we introduce the zooming coordinates of Bouquet et al. (1985) to solve equations (1) through (4). The zooming coordinates, $(\boldsymbol{\xi}, \tau)$, are related with the ordinary coordinates, (\mathbf{r}, t) , by

$$\begin{pmatrix} \boldsymbol{\xi} \\ \tau \end{pmatrix} = \begin{pmatrix} \frac{\mathbf{r}}{c_0 |t - t_0|} \\ -\ln |1 - t/t_0| \end{pmatrix}, \quad (5)$$

where c_0 denotes a standard sound speed and is a function of time t . The symbol, t_0 , denotes an epoch at the instant of the protoneutron star formation. The density in the zooming coordinates, ϱ , is related with that in the ordinary coordinates, ρ , by

$$\varrho(\mathbf{x}, \tau) = 4\pi G\rho(t - t_0)^2. \quad (6)$$

We define the standard sound speed, c_0 , so that it denotes the sound speed at a given t when $\varrho = 1$. Thus it is expressed as

$$c_0 = \sqrt{\gamma K} (4\pi G)^{(1-\gamma)/2} |t - t_0|^{1-\gamma}. \quad (7)$$

The pressure in the zooming coordinates, p , is related with the that in the ordinary coordinates, P , by

$$p = \frac{4\pi G}{c_0^2} P(t - t_0)^2. \quad (8)$$

Substituting equations (6) and (8) into equation (1), we obtain the polytrope relation in the zooming coordinates,

$$p = \frac{\varrho^\gamma}{\gamma}. \quad (9)$$

The velocity in the zooming coordinates, \mathbf{u} , is defined as

$$\mathbf{u} = \frac{\mathbf{v}}{c_0} + (2 - \gamma) \frac{\mathbf{r}}{c_0 |t - t_0|}. \quad (10)$$

This velocity denotes that with respect to the zooming coordinates, and includes the apparent motion, the last term in equation (10). The gravitational potential in the zooming coordinates, ϕ , is related with that in the ordinary coordinates, Φ by

$$\phi = \frac{\Phi}{c_0^2}. \quad (11)$$

In the zooming coordinates, the hydrodynamical equations are expressed as

$$\frac{\partial \varrho}{\partial \tau} + \nabla_{\boldsymbol{\xi}} \cdot (\varrho \mathbf{u}) = (4 - 3\gamma) \varrho, \quad (12)$$

$$\frac{\partial}{\partial \tau}(\varrho \mathbf{u}) + \nabla_{\xi} \cdot (\varrho \mathbf{u} \otimes \mathbf{u}) + \nabla_{\xi} p + \varrho \nabla_{\xi} \phi = (2 - \gamma)(\gamma - 1) \varrho \xi + (7 - 5\gamma) \varrho \mathbf{u}, \quad (13)$$

and

$$\Delta_{\xi} \phi = \varrho \quad (14)$$

for $t < t_0$. The symbols, ∇_{ξ} and Δ_{ξ} , denote the gradient and Laplacian in the ξ -space, respectively.

Assuming stationarity in the zooming coordinates ($\partial/\partial \tau = 0$) and spherical symmetry ($\partial/\partial \theta = \partial/\partial \varphi = 0$), we seek a similarity solution. Under these assumptions equations (12), (13), and (14) reduce to

$$\frac{\partial u_r}{\partial \xi} + \frac{u_r}{\varrho} \frac{\partial \varrho}{\partial \xi} = (4 - 3\gamma) - \frac{2u_r}{\xi}, \quad (15)$$

$$u_r \frac{\partial u_r}{\partial \xi} + \frac{1}{\varrho} \left(\frac{dp}{d\varrho} \right) \frac{\partial \varrho}{\partial \xi} + \frac{\partial \phi}{\partial \xi} = (2 - \gamma)(\gamma - 1) \xi + (3 - 2\gamma) u_r, \quad (16)$$

and

$$\frac{\partial \phi}{\partial \xi} = \frac{1}{\xi^2} \int_0^{\xi} \varrho(\zeta) \zeta^2 d\zeta = \frac{\varrho u_r}{4 - 3\gamma}, \quad (17)$$

where $\xi = |\xi|$. After some algebra we can rewrite equations (15) and (16) into

$$(\varrho^{\gamma-1} - u_r^2) \left(\frac{d\varrho}{d\xi} \right) = \varrho \left[-\frac{\varrho u_r}{4 - 3\gamma} + (2 - \gamma)(\gamma - 1) \xi + (\gamma - 1) u_r + \frac{2u_r^2}{\xi} \right], \quad (18)$$

and

$$\begin{aligned} (\varrho^{\gamma-1} - u_r^2) \left(\frac{du_r}{d\xi} \right) &= \frac{\varrho u_r^2}{4 - 3\gamma} - (2 - \gamma)(\gamma - 1) \xi u_r - (3 - 2\gamma) u_r^2 \\ &+ (4 - 3\gamma) \varrho^{\gamma-1} - \frac{2u_r}{\xi} \varrho^{\gamma-1}. \end{aligned} \quad (19)$$

Equations (18) and (19) are singular at the sonic point, $u_r^2 = \varrho^{\gamma-1}$. We obtain the the similarity solution by integrating equations (18) and (19) with the Runge-Kutta method. In the numerical integration we used the auxiliary variable of Whitworth & Summers (1985), s , defined by

$$\frac{d\xi}{ds} = \varrho^{\gamma-1} - u_r^2. \quad (20)$$

Using equation (20), we rewrite equations (18) and (19) into

$$\frac{d\varrho}{ds} = \varrho \left[-\frac{\varrho u_r}{4 - 3\gamma} + (2 - \gamma)(\gamma - 1) \xi + (\gamma - 1) u_r + \frac{2u_r^2}{\xi} \right], \quad (21)$$

and

$$\begin{aligned} \frac{du_r}{ds} &= \frac{\varrho u_r^2}{4 - 3\gamma} - (2 - \gamma)(\gamma - 1) \xi u_r - (3 - 2\gamma) u_r^2 \\ &+ (4 - 3\gamma) \varrho^{\gamma-1} - \frac{2u_r}{\xi} \varrho^{\gamma-1}, \end{aligned} \quad (22)$$

respectively.

Similarity solutions exist for $\gamma < 4/3$. Figure 1 shows the similarity solution for $\gamma = 1.3$. The solid curves denote ϱ while the dashed curves denote the infall velocity, $-v_r = -u_r + (2 - \gamma)\xi$. These solutions are the same as those obtained by Yahil (1983) and Suto & Silk (1988). They have the asymptotic forms of

$$\varrho_0 = \varrho_c - \frac{\varrho_c^{2-\gamma}}{6} \left(\varrho_c - \frac{2}{3} \right) \xi^2 + \mathcal{O}(\xi^4), \quad (23)$$

and

$$\mathbf{u}_0 = \left[\left(\frac{4}{3} - \gamma \right) \xi + \frac{\varrho_c^{1-\gamma}}{15} \left(\varrho_c - \frac{2}{3} \right) \left(\frac{4}{3} - \gamma \right) \xi^3 + \mathcal{O}(\xi^5) \right] \mathbf{e}_\xi. \quad (24)$$

The value of ϱ_c is 22.04 for $\gamma = 1.3$.

3. VORTEX MODE

In this section we consider a non-spherical perturbation around the similarity solution. The density perturbation is assumed to be proportional to the spherical harmonics, $Y_\ell^m(\theta, \varphi)$. Then the density and velocity are expressed as

$$\varrho = \varrho_0 + \delta\varrho(\xi) e^{\sigma\tau} Y_\ell^m(\theta, \varphi), \quad (25)$$

$$u_r = u_{r0} + \delta u_r(\xi) e^{\sigma\tau} Y_\ell^m(\theta, \varphi), \quad (26)$$

$$u_\theta = \delta u_\theta(\xi) \frac{e^{\sigma\tau}}{\ell + 1} \frac{\partial}{\partial\theta} Y_\ell^m(\theta, \varphi), \quad (27)$$

$$u_\varphi = \delta u_\theta(\xi) \frac{e^{\sigma\tau}}{(\ell + 1) \sin\theta} \frac{\partial}{\partial\varphi} Y_\ell^m(\theta, \varphi), \quad (28)$$

$$\phi = \phi_0 + \delta\phi(\xi) e^{\sigma\tau} Y_\ell^m(\theta, \varphi), \quad (29)$$

where the symbols with suffix, 0, denote the values in the similarity solution and the symbols with the symbol, δ , denote the perturbations. Substituting equations (26) throughout (29) into equations (12), (13), and (14), we obtain the perturbation equations,

$$(\sigma + 3\gamma - 4) \delta\varrho + \frac{1}{\xi^2} \frac{\partial}{\partial\xi} [\xi^2 (\varrho_0 \delta u_r + u_{r0} \delta\varrho)] - \ell \frac{\varrho_0 \delta u_\theta}{\xi} = 0, \quad (30)$$

$$(\sigma + 2\gamma - 3) \delta u_r + \frac{\partial}{\partial\xi} (u_{r0} \delta u_r) + \frac{\partial}{\partial\xi} \left(\frac{\delta\varrho}{\varrho_0^{2-\gamma}} \right) + \delta\Gamma = 0, \quad (31)$$

$$(\sigma + 2\gamma - 3) \delta u_\theta + \frac{u_{r0}}{\xi} \frac{\partial}{\partial\xi} (\xi \delta u_\theta) + \frac{\ell + 1}{\xi} \left(\frac{\delta\varrho}{\varrho_0^{2-\gamma}} + \delta\phi \right) = 0, \quad (32)$$

$$\frac{\partial}{\partial\xi} \delta\phi = \delta\Gamma, \quad (33)$$

and

$$\frac{\partial}{\partial \xi} \delta \Gamma = -\frac{2 \delta \Gamma}{\xi} + \frac{\ell(\ell+1)}{\xi^2} \delta \phi + \delta \varrho. \quad (34)$$

These perturbation equations have singularities at the origin ($\xi = 0$), the sonic point $[(u_{r0})^2 - \varrho^{\gamma-1}]$, and the infinity ($\xi = +\infty$). These perturbation equations are the same as those of Hanawa & Matsumoto (2000).

To obtain the boundary condition at the origin we use the Taylor expansion of the perturbation. In the following we use the notation,

$$\frac{\delta \varrho}{\varrho_0^{2-\gamma}} = \varepsilon_0 \xi^\ell + \varepsilon_2 \xi^{\ell+2} + \mathcal{O}(\xi^{\ell+4}), \quad (35)$$

$$\delta u_r = \alpha_0 \xi^{\ell-1} + \alpha_2 \xi^{\ell+1} + \mathcal{O}(\xi^{\ell+3}), \quad (36)$$

$$\delta u_\theta = \beta_0 \xi^{\ell-1} + \beta_2 \xi^{\ell+1} + \mathcal{O}(\xi^{\ell+3}), \quad (37)$$

and

$$\delta \phi = \lambda_0 \xi^\ell + \lambda_2 \xi^{\ell+2} + \mathcal{O}(\xi^{\ell+4}). \quad (38)$$

Substituting equation (38) into equation (33) we obtain

$$\delta \Gamma = \ell \lambda_0 \xi^{\ell-1} + (\ell+2) \lambda_2 \xi^{\ell+1} + \mathcal{O}(\xi^{\ell+3}). \quad (39)$$

Note that not only the leading terms but the second lowest terms are taken into account in equations (35) through (39).

Substituting equations (35) through (39) into equations (30) through (34) we derive conditions for α_0 , α_2 , β_0 , β_2 , ε_0 , ε_2 , λ_0 , and λ_2 . From equation (30) we obtain

$$(\ell+1) \alpha_0 - \ell \beta_0 = 0. \quad (40)$$

Equation (40) ensures that the terms proportional to $\xi^{\ell-2}$ vanish in equation (30). The terms proportional to $\xi^{\ell-2}$ vanish in equation (34) at any condition. From equations (31) and (32) we obtain

$$\left[\sigma + 2\gamma - 3 + \ell \left(\frac{4}{3} - \gamma \right) \right] \alpha_0 + \ell(\varepsilon_0 + \lambda_0) = 0, \quad (41)$$

and

$$\left[\sigma + 2\gamma - 3 + \ell \left(\frac{4}{3} - \gamma \right) \right] \beta_0 + (\ell+1)(\varepsilon_0 + \lambda_0) = 0, \quad (42)$$

respectively. These equations ensure that the terms proportional to $\xi^{\ell-1}$ vanish in equations (27) and (28). Similarly we obtain

$$\begin{aligned} & \varrho_c^{2-\gamma} \left[\sigma + \ell \left(\frac{4}{3} - \gamma \right) \right] \varepsilon_0 + \varrho_c [(\ell+3) \alpha_2 - \ell \beta_2] \\ & - \frac{\varrho_c^{2-\gamma}}{6} \left(\varrho_c - \frac{2}{3} \right) [(\ell+3) \alpha_0 - \ell \beta_0] = 0, \end{aligned} \quad (43)$$

and

$$[(\ell + 2)(\ell + 3) - \ell(\ell + 1)]\lambda_2 = \varrho_c^{2-\gamma}\varepsilon_0, \quad (44)$$

from the condition that the terms proportional to ξ^ℓ vanish and

$$\begin{aligned} \left[\sigma + 2\gamma - 3 + (\ell + 2) \left(\frac{4}{3} - \gamma \right) \right] \alpha_2 + (\ell + 2) \frac{\varrho_c^{1-\gamma}}{15} \left(\varrho_c - \frac{2}{3} \right) \left(\frac{4}{3} - \gamma \right) \alpha_0 \\ + (\ell + 2)(\varepsilon_2 + \lambda_2) = 0, \end{aligned} \quad (45)$$

and

$$\begin{aligned} \left[\sigma + 2\gamma - 3 + (\ell + 2) \left(\frac{4}{3} - \gamma \right) \right] \beta_2 + \ell \frac{\varrho_c^{1-\gamma}}{15} \left(\varrho_c - \frac{2}{3} \right) \left(\frac{4}{3} - \gamma \right) \beta_0 \\ + (\ell + 1)(\varepsilon_2 + \lambda_2) = 0 \end{aligned} \quad (46)$$

from the condition that the terms proportional to $\xi^{\ell+1}$ vanish.

From equations (40), (45) and (46) we obtain

$$\left[\sigma + 2\gamma - 3 + (\ell + 2) \left(\frac{4}{3} - \gamma \right) \right] [(\ell + 1)\alpha_2 - (\ell + 2)\beta_2] = 0. \quad (47)$$

This condition is equivalent to the condition that either of

$$(\ell + 1)\alpha_2 - (\ell + 2)\beta_2 = 0 \quad (48)$$

and

$$\sigma = \frac{1}{3} + \ell \left(\gamma - \frac{4}{3} \right) \quad (49)$$

is fulfilled. The bar mode found by Hanawa & Matsumoto (2000) fulfills equation (48). We seek the other mode that fulfills equation (49). In the following we call the latter the vortex mode.

Since the perturbation is linear, the solution can be arbitrarily scaled. To normalize the solution we take $\alpha_0 = 1$ in this paper. Then we obtain

$$\beta_0 = \frac{\ell + 1}{\ell}, \quad (50)$$

$$\lambda_0 = -\varepsilon_0 + \frac{2}{\ell} \left(\frac{4}{3} - \gamma \right), \quad (51)$$

$$\varepsilon_0 = -3\varrho_c^{\gamma-1} [(\ell + 3)\alpha_2 - \ell\beta_2] + \left(\varrho_c - \frac{2}{3} \right), \quad (52)$$

$$\lambda_2 = \frac{\varrho_c^{2-\gamma}}{2(2\ell + 3)}\varepsilon_0, \quad (53)$$

and

$$\varepsilon_2 = -\frac{\varrho_c^{1-\gamma}}{15} \left(\varrho_c - \frac{2}{3} \right) \left(\frac{4}{3} - \gamma \right) - \lambda_2. \quad (54)$$

We obtained an eigenfunction of this vortex mode numerically by the following procedures. First we integrated equations (21) and (22) to obtain the similarity solution for a given γ . Second we obtained three linearly independent solutions for the perturbation around the origin by using the Taylor series expansion, equations (35) through (39). Third we integrated the three linearly independent solutions from the origin toward the sonic point numerically with the Runge-Kutta method. Forth we obtained two linearly independent solutions satisfying the boundary conditions both at the origin and sonic point by taking linear combinations of the numerically integrated solutions. Finally we integrated the two linearly independent solutions from the sonic point toward the infinity and obtained an eigenfunction satisfying all the boundary conditions as a linear combination of them. The eigenfunction should have an infinitesimal small amplitude at the infinity as shown in Appendix.

Figures 2, 3, and 4 denote the numerically obtained eigenfunctions of $\ell = 1, 2,$ and $3,$ respectively. The polytropic index is set to be $\gamma = 1.3$ in the figures. The eigenfunctions are normalized so that the radial velocity perturbation is $\delta u_r = \xi^{\ell-1} + \mathcal{O}(\xi^{\ell+1})$ near the origin. The non-radial velocity perturbation, $\delta u_\theta,$ changes its sign around $\xi \approx 1.$ The density perturbation is small. It should be proportional to $(\gamma - 4/3)$ [see eq. (51)].

The vortex mode of $\ell = 1$ is different from the ghost mode of $\ell = 1$ (Hanawa & Matsumoto 1999, 2000). The vortex mode denotes circulation streaming back through the core surface while the ghost mode denotes misfit of the gravity center to the coordinate center (Hanawa & Matsumoto 1999). The ghost mode has no vortex ($\nabla_\xi \times \delta \mathbf{u} = 0$). The vortex mode of $\ell = 1$ has the growth rate of $\sigma = \gamma - 1$ while the ghost mode has that of $\sigma = 2 - \gamma.$

Figure 5 shows the density and velocity perturbation in the cross section. The contours denote the iso-density curves of $\varrho = 10, 3, 1, 0.3,$ and 0.1 while the central density is $\varrho_c = 22.04.$ The arrows denote the velocity vectors. We obtained the density and velocity by adding the eigenmode of $(\ell, m) = (2, 0)$ on the similarity solution for $\gamma = 1.3.$ The infall is a little faster in the x -direction than in the z -direction. Figure 6 is the same as Figure 5 but only the velocity perturbation is shown by the arrows in Figure 6. It shows that this eigenmode is an vortex flow in the meridional plane.

4. GROWTH MECHANISM

In this section we discuss the mechanism for the growth of the vortex mode. We consider the conservation of vorticity to elucidate the growth mechanism. Taking rotation of the equation of motion, we obtain,

$$\frac{\partial \Omega}{\partial t} = \nabla \times (\mathbf{v} \times \Omega), \quad (55)$$

where

$$\Omega = \nabla \times \mathbf{v}, \quad (56)$$

since the rotation of the pressure force and that of gravity vanish. Similarly the conservation of the vorticity is expressed as

$$\frac{\partial \boldsymbol{\omega}}{\partial \tau} = \nabla_{\xi} \times (\mathbf{u} \times \boldsymbol{\omega}) + (3 - 2\gamma) \boldsymbol{\omega} , \quad (57)$$

where

$$\boldsymbol{\omega} = \nabla_{\xi} \times \mathbf{u} . \quad (58)$$

Since $\nabla_{\xi} \times \mathbf{u}_0 = 0$, we obtain

$$\frac{\partial}{\partial \tau} \delta \boldsymbol{\omega} = \nabla_{\xi} \times (\mathbf{u}_0 \times \delta \boldsymbol{\omega}) + (3 - 2\gamma) \delta \boldsymbol{\omega} , \quad (59)$$

for the perturbation of the vortex, $\delta \boldsymbol{\omega}$. Substituting the equation (24) into equation (59) we obtain

$$\frac{\partial}{\partial \tau} \delta \boldsymbol{\omega} = \left[\left(\gamma - \frac{4}{3} \right) \frac{\partial}{\partial \ln \xi} + \frac{1}{3} \right] \delta \boldsymbol{\omega} , \quad (60)$$

near $\xi = 0$. We can derive equation (49) from equation (60) since $\delta \boldsymbol{\omega} \propto \xi^{\ell}$ near $\xi = 0$ in the vortex mode. We can derive also the growth rate of the spin-mode, $\sigma = 1/3$, from equation (60) since $\delta \boldsymbol{\omega} = \xi^0$ near $\xi = 0$ in the spin-up mode. The growth of the vortex mode as well as that of the spin-up mode is subject to the conservation of the vorticity.

5. IMPLICATION TO TYPE II SUPERNOVA

As shown in the previous sections the vortex mode grows in proportion to $|t - t_0|^{-\sigma}$. In other words it grows in proportion to $\rho_c^{\sigma/2}$ since $\rho_c \propto (t - t_0)^{-2}$. This growth rate is for the growth of the relative amplitude, i.e., that for $\delta u = \delta v/c_0$. The growth of the anisotropic velocity is proportional to

$$\delta v \propto c_0 \rho_c^{\sigma/2} \propto \rho_c^{\sigma'} , \quad (61)$$

where

$$\sigma' = \frac{1}{3} + \frac{\ell + 1}{2} \left(\gamma - \frac{4}{3} \right) . \quad (62)$$

Suppose that an iron core during implosion can be well approximated by a polytrope of $\gamma = 1.3$. Then the velocity perturbation of $\ell = 1$ grows by a factor of 30 while the density increases from $\rho_c = 10^9 \text{ g cm}^{-3}$ to $10^{14} \text{ g cm}^{-3}$. Similarly that of $\ell = 2$ grows by a factor of 25 during the same period.

If the $\ell = 1$ mode is amplified, the central core, i.e., the proton-neutron star has a bulk velocity relative to the envelope. This might explain a run-away pulsar from its natal nebula. If the $\ell \geq 2$ mode is amplified, the anisotropic velocity will cause global mixing during the supernova explosion ($t > t_0$). This may explain heavy element exposure earlier than expected from a spherical symmetric model.

It should be also noted that the vortex mode of $(\ell, m) = (2, 0)$ has velocity field similar to that of the Eddington-Sweet meridional circulation. If a pre-supernova star rotates slowly, the meridional circulation can be a seed of the vortex mode amplified during the implosion phase. Convection during Si-burning may also be the seed for the vortex mode.

We thank Shigehiro Nagataki, Katsuhiko Sato, and Shoichi Yamada for helpful discussion. This research is financially supported in part by the Grant-in-Aid for Scientific Research on Priority Areas of the Ministry of Education, Science, Sports and Culture of Japan (No. 10147105, 11134209).

A. Asymptotic Behavior around the Infinity

In this appendix we derive asymptotic forms of perturbations around the similarity solution for a collapsing gas sphere. In the region of $\xi \gg 1$ the similarity solution has the asymptotic form of

$$\varrho \propto \xi^{-2/(2-\gamma)}, \quad (\text{A1})$$

and

$$[u_r - (2 - \gamma)\xi] \propto \xi^{(1-\gamma)/(2-\gamma)}. \quad (\text{A2})$$

See Yahil (1983) and Suto & Silk (1988) for the derivation.

As a boundary condition we assume that the relative density perturbation, $\delta\varrho/\varrho_0$, is vanishingly small at infinity, $\xi = \infty$. After some algebra we obtain the asymptotic relations,

$$\frac{\delta\varrho}{\varrho_0} \propto \xi^{-\sigma/(2-\gamma)} \quad (\text{A3})$$

$$\delta u_r \propto \xi^{-(\sigma+\gamma-1)/(2-\gamma)}, \quad (\text{A4})$$

$$\delta u_\theta \propto \xi^{-(\sigma+\gamma-1)/(2-\gamma)}, \quad (\text{A5})$$

$$\phi \propto \xi^{-(\sigma-2\gamma+2)/(2-\gamma)}, \quad (\text{A6})$$

and

$$\phi = \left[\frac{(\sigma - 2\gamma + 2)(\sigma - 3\gamma + 4)}{(2 - \gamma)^2} - \ell(\ell + 1) \right]^{-1} r^2 \delta\varrho. \quad (\text{A7})$$

When we derive the above relations, we use equations (A1) and (A2). See also Hanawa & Matsumoto (2000) for the derivation.

REFERENCES

- Arnett, W. D., Fryxell, B. A., & Müller, E. 1989, *ApJ*, 341, L63
 Bethe, H. A. 1990, *Rev. Mod. Phys.*, 62, 801

- Bouquet, S., Feix, M. R., Fijalkow, E., & Munier, A. 1985, *ApJ*, 293, 494
- Burrows, A., & Hayes, J. 1996, *Phys. Rev. Lett.*, 76, 352
- Falk, S. W., & Arnett, W. D. 1973, *ApJ*, 180, L65
- Goldreich, P., Lai, D., & Sahrling, M. 1977, in *Unsolved Problems in Astrophysics*, ed. J. N. Bahcall & J. P. Ostriker (Princeton, Princeton Univ. Press), 269
- Hachisu, I., Matsuda, T., Nomoto, K., & Shigeyama, T. 1990, *ApJ*, 358, L57
- Hanawa, T., & Matsumoto, T. 1999, *ApJ*, 521, 703
- , *PASJ*, 52, in press
- Hanawa, T., & Nakayama, K. 1997, *ApJ*, 484, 238
- Müller, E., Fryxell, B. A., & Arnett, W. D. 1991, *Å*, 103, 358
- Nagataki, S., Shimizu, T. M., & Sato, K. *ApJ*, 495, 413
- Suto, Y., & Silk, J. 1988, *ApJ*, 326, 527
- Whitworth, A., & Summers, D. 1985, *MNRAS*, 214, 1
- Yahil, A. 1983, *ApJ*, 265, 1047

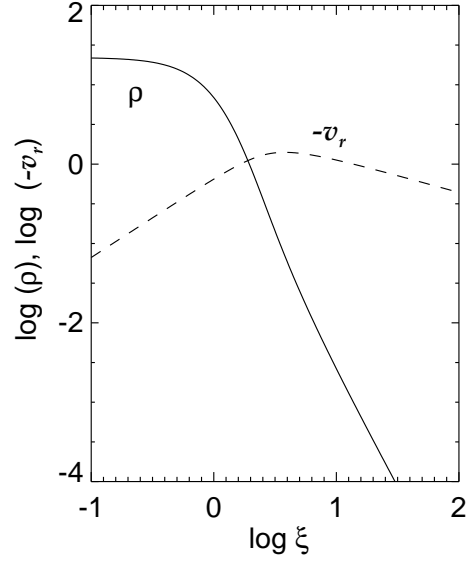


Fig. 1.— The similarity solution is shown for a collapsing polytropic gas sphere of $\gamma = 1.30$. The solid curves denote the density, $\rho(\xi)$, and the infall velocity, $-v_r(\xi) \equiv (2 - \gamma)\xi - u_r(\xi)$. The latter is normalized by the sound speed at the center.

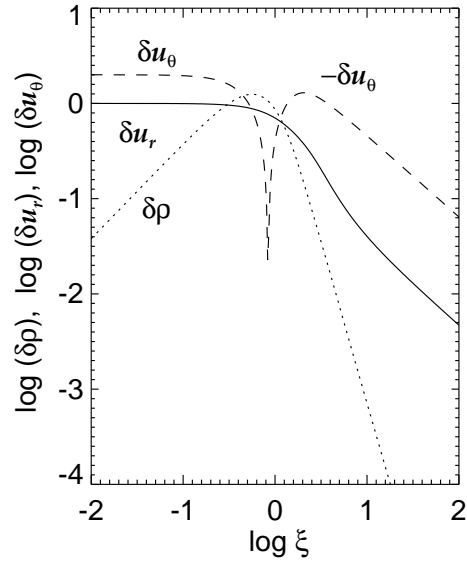


Fig. 2.— The eigenfunction of $\ell = 1$ mode is shown as a function of ξ . The solid curve denotes the radial velocity perturbation, δu_r . The dashed and dotted curves denote δu_θ and $\delta\rho$, respectively.

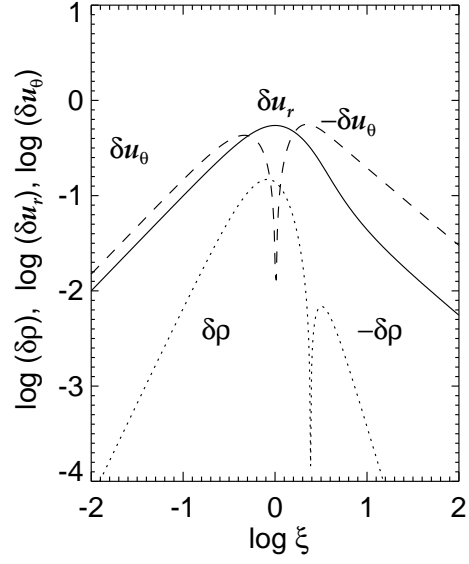


Fig. 3.— The same as Figure 1 but for $\ell = 2$ mode.

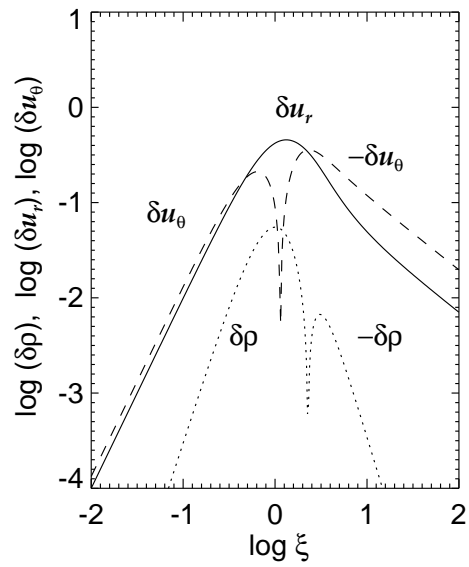


Fig. 4.— The same as Figure 2 but for $\ell = 3$ mode.

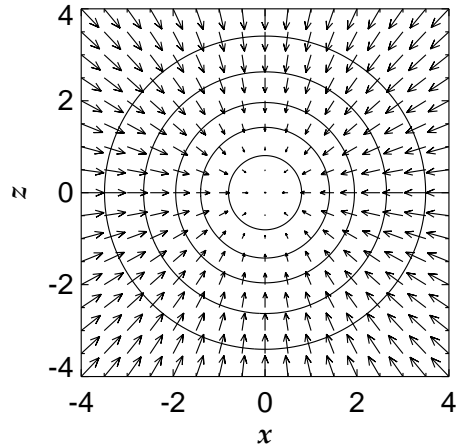


Fig. 5.— This cross section shows a dynamically collapsing iron core suffering the vortex mode of $\ell = 2$. The contours denote the isodensity curves of $\rho = 10.0, 3.0, 1.0, 0.3,$ and 0.1 . The arrows denote the velocity, \mathbf{v} , in the $x - z$ plane.

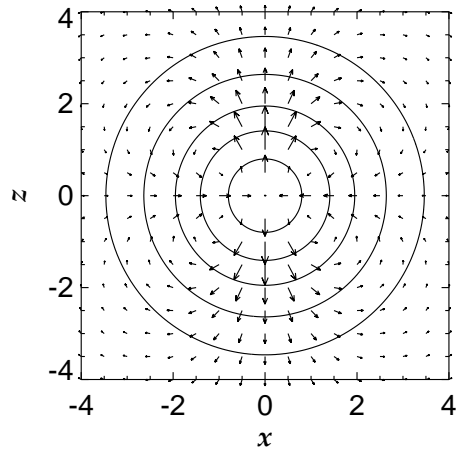


Fig. 6.— The same as Figure 4 but only the velocity perturbation is shown by the arrows.